communications biology

A Nature Portfolio journal

Article

https://doi.org/10.1038/s42003-025-08613-8

rTMS ameliorates cerebral ischemia-reperfusion injury by inhibiting Golgi apparatus stress through epigenetic modulation of Gli2

Chunjiao Zhu, Yongmei Fan & Wenna Peng

Cerebral ischemic stroke represents a primary cause of permanent disability and mortality globally. Repetitive transcranial magnetic stimulation (rTMS) has emerged as a prominent focus in treating a wide range of neurological disorders. In this study, we explore the role of rTMS in alleviating cerebral ischemia-reperfusion (I/R) injury by mediating Golgi apparatus (GA) stress. Here, we find that rTMS upregulates Dram1 expression and ameliorates GA stress in cerebral I/R injury in vivo and in vitro. Gli2 transcriptionally activates Dram1. HDAC5 inhibits H3K27ac modification of Gli2 promoter. rTMS promotes Gli2 expression by inhibiting HDAC5. Gli2 knockdown reverses the inhibitory effect of rTMS on OGD/R-induced neuronal GA stress. In conclusion, rTMS inhibits HDAC5-mediated deacetylation of Gli2 promoter to promote the transcriptional activation of Dram1, thereby suppressing cerebral I/R-induced GA stress. Targeting Gli2/ Dram1 axis may be an effective way to enhance the anti-ischemic stroke effect of rTMS.

Cerebral ischemic stroke is a leading cause of permanent disability and mortality worldwide, posing a significant threat to human health[1,2]. Currently, thrombolytic therapy, which restores blood flow, is the primary treatment for cerebral ischemic stroke[1,3]. Nevertheless, reperfusion can paradoxically cause additional damage to ischemic tissues, known as cerebral ischemia-reperfusion (I/R) injury[4]. This secondary damage is associated with neuronal death and can result in impaired cognitive function, disability, and even death[5,6]. Therefore, effective prevention and treatment of cerebral I/R injury is crucial for mitigating the impact of cerebral ischemic stroke.

The pathogenetic mechanism underlying cerebral I/R injury involves a complex network of factors, including oxidative stress, calcium overload, and immune inflammation. Oxidative stress is regarded as a central therapeutic target[5,7,8]. The Golgi apparatus (GA), an organelle closely associated with cell death, plays a role in the oxidative stress response[9,10]. During oxidative stress, GA undergoes a series of changes such as deformation and fragmentation, collectively termed the GA stress response[7]. Damaged GA extensively accumulated in neurons following cerebral ischemia or ischemic death[5]. A previous study demonstrated that the GA stress response was significantly enhanced in oxygen-glucose deprivation/reoxygenation (OGD/R)-induced cerebral I/R injury[7]. Moreover, inhibiting the down-regulation of Ca^{2+}-ATPase isoform 1 alleviated GA stress and consequently reduced cerebral I/R injury[11]. Therefore, inhibition of the GA stress response may represent a promising strategy for mitigating cerebral I/R injury.

Recently, repetitive transcranial magnetic stimulation (rTMS) has obtained significant attention in clinical applications of neuroscience research owing to its proven efficacy in treating a wide range of neurological disorders, including depression, anxiety, and Parkinson's disease[12,13]. Emerging evidence has highlighted its fundamental role in ischemic cerebrovascular diseases[14]. For instance, rTMS facilitated stroke recovery by protecting blood vessels and promoting neovascularization[15]. Moreover, it improved motor function in cerebral ischemic mice by inhibiting neuronal focal death and modulating microglial polarization[16]. Additionally, rTMS alleviated oxidative stress and neuropathy in rats with cerebral infarction by modulating the nuclear factor erythroid-derived 2-like 2 (Nrf2) pathway[14]. However, whether rTMS affects cerebral I/R injury by modulating the GA stress response has not been reported.

Histone deacetylases (HDACs) function as enzymes that modulate histone acetylation dynamics within cells, collaborating with histone acetyltransferases to preserve optimal histone acetylation homeostasis and thereby governing gene expression[17]. HDACs are widely expressed in the nervous system, and their abnormal activity is closely linked to various neurodegenerative diseases[18]. HDACs are classified into 4 classes and 18 isoforms according to their sequence, structure, and functional homology[19].

Department of Rehabilitation, Second Xiangya Hospital of Central South University, Changsha, Hunan, 410011, China. e-mail: pengwenna@csu.edu.cn

Among these, HDAC5 belongs to the class II HDAC subfamily and is extensively expressed in brain tissues[18]. Studies proved that HDAC5 expression was increased in rat brain tissues during I/R injury[20]. HDAC5 overexpression impaired the protective potential of dexmedetomidine in OGD-treated neurons[21]. Notably, one study showed that rTMS induced sustained histone acetylation in prefrontal cortex of mice[22]. Therefore, rTMS may mitigate cerebral I/R injury by modulating relevant histone acetylation.

Glioma-associated oncogene protein 2 (Gli2), a member of the GLI family of zinc finger proteins, primarily functions as a transcriptional activator and plays a crucial role in brain development and neurogenesis[23]. Gli2 has recently been shown to promote the proliferation and differentiation of neural stem cells[24]. Additionally, Gli2 expression has been reported to be reduced in OGD/R cells, whereas its overexpression mitigates I/R-induced brain damage in mice[25]. The transcriptional activity of *Gli2* is typically inhibited by histone deacetylation. Chen et al.[26] revealed that granule neuron precursor neurogenesis and cerebellar development could be regulated by inhibiting the interaction between *Gli2* and histone acetyltransferase. Importantly, HDAC5 interacted with *Gli2*, and HDAC5 recruitment repressed the transcriptional activity of *Gli2*[27]. However, the specific effects of rTMS on *Gli2* transcription remain unclear.

DNA damage-regulated autophagy modulator 1 (Dram1) is a multichannel lysosomal membrane protein that plays crucial roles in regulating various cellular processes, including autophagy, cell death, immunity, and differentiation[28]. Dram1 protected neuroblastoma cells from OGD/R-induced injury by regulating autophagy[29]. Wei et al.[30] revealed that Dram1 knockdown led to GA stress and disrupted GA-associated vesicle transport, suggesting that Dram1 may play an important role in regulating GA stress. Gli2 was demonstrated to transcriptionally activate *lncRNA Peg13*, which inhibited apoptosis and oxidative stress in OGD/R-treated murine brain microvascular endothelial cells[25]. However, it remains unclear whether Gli2 transcriptionally activates *Dram1* to modulate neuronal GA stress during cerebral I/R injury.

This study explored the molecular mechanisms through which rTMS regulated GA stress and nerve cell injury during cerebral ischemic stroke in vivo and in vitro. We hypothesized that rTMS could alleviate GA stress in cerebral I/R injury by manipulating *Gli2* epigenetic modulation via HDAC5 inhibition and boosting the transcriptional activity of *Dram1*. This study aimed to establish a theoretical rationale for the potential therapeutic role of rTMS in mitigating cerebral I/R injury and to develop a novel treatment strategy for this condition.

Results

rTMS ameliorated GA stress and brain injury in middle cerebral artery occlusion/reperfusion (MCAO/R) mice

To explore the effect of rTMS on cerebral I/R injury, we treated MCAO/R mice with rTMS. The experimental paradigm was shown in Fig. 1A. As shown in Fig. 1B, compared to the control and sham groups, the percentage of infarct area in brain tissues was dramatically increased in the MCAO/R group, whereas rTMS decreased the percentage of infarct area in MCAO/R mice. Higher modified neurological severity score (mNSS) signified more severe neurological impairments[7]. Additionally, MCAO/R mice exhibited increased mNSS, whereas further treatment with rTMS reduced the mNSS (Fig. 1C). Furthermore, brain water content was markedly increased in MCAO/R mice; however, mice treated with rTMS showed a significant decrease in brain water content compared with the MCAO/R group (Fig. 1D). TUNEL staining showed that MCAO/R treatment enhanced neuronal apoptosis in the cortical and hippocampal regions of the mouse brain tissues, whereas rTMS ameliorated neuronal apoptosis (Fig. 1E, F). Importantly, we also observed that MCAO/R induced neuronal damage in the cortical and hippocampal regions of the mice, but rTMS inhibited this damage (Fig. 1G, H). GA stress occurs under cerebral ischemic condition, causing damage to the GA structure and function, which plays an important role in exacerbating ischemic brain injury[5]. Given that modulation of GA stress is an important strategy for alleviating cerebral ischemic injury, we further explore whether rTMS plays an ameliorative role by modulating GA stress. In MCAO/R mice, the levels of GA structure and function-related proteins, such as Golgi phosphoprotein 3 (GOLPH3), ADP-ribosylation factor 4 (ARF4), and Acyl-CoA-binding domain-containing 3 (ACBD3) were increased, while the protein levels of Golgi matrix protein 130 (GM130) and secretory pathway Ca^{2+}/Mn^{2+}-ATPase pump type 1 (SPCA1) were decreased. However, rTMS reversed the changes of above GA functional and structural proteins (Figure S1A). MCAO/R treatment resulted in the increased level of GA stress sensor GOLPH3 in neurons of the cortex and hippocampus regions, whereas this colocalization was attenuated after rTMS treatment (Figure S1B, C). In addition, in the MCAO/R group, the GA exhibited significant morphological alterations, characterized by swelling, fragmentation, a reduced number of cisternae within each stack, and an increased number of vesicles. rTMS mitigated MCAO/R-induced GA fragmentation, promoting the gradual restoration of the GA to its normal structure (Figure S1D, E). Therefore, rTMS alleviated the GA stress and brain damages in MCAO/R mice.

rTMS suppressed OGD/R-induced GA stress and neuronal damage by upregulating Dram1

At the cellular level, we simulated cerebral I/R injury in vitro by treating cells with OGD/R and investigated the effects of 1, 5, 10, 15, and 20 Hz rTMS on OGD/R cells. The viability of both primary neurons and N2a cells in OGD/R group was clearly diminished compared to that in the control group. However, rTMS enhanced the neuronal cell viability in a dose-dependent manner. Specifically, 10 and 15 Hz rTMS showed similar and optimal effects, whereas increasing the frequency to 20 Hz resulted in a less pronounced improvement (Fig. 2A). It is known that the LDH release increases when cells are damaged or died[31]. OGD/R treatment increased LDH release in primary neurons and N2a cells, but rTMS inhibited LDH release in a dose-dependent manner, with 10 and 15 Hz having the best effects (Fig. 2B). Furthermore, rTMS alleviated OGD/R-induced apoptosis (Fig. 2C, D). Dram1 is a key factor in maintaining normal GA structure[5]. Notably, in MCAO/R mice, Dram1 mRNA and protein levels were reduced, and this effect was reversed by rTMS (Figure S2A, B). OGD/R treatment also reduced Dram1 mRNA and protein levels in primary neurons and N2a cells, which were increased by rTMS (Fig. 2E, F). Based on these results, rTMS at 10 Hz and 15 Hz had the best and similar therapeutic effect. Therefore, 10 Hz rTMS was selected for subsequent experiments. Regarding GA functional and structural proteins, OGD/R treatment significantly upregulated the levels of GOLPH3, ARF4, and ACBD3, and downregulated the levels of GM130 and SPCA1, and 10 Hz rTMS reversed these changes of above protein levels in primary neurons and N2a cells (Fig. 2G). Transmission electron microscopy revealed the typical banded structure of GA in normal primary neurons and N2a cells. However, in the OGD/R group, the GA displayed marked morphological abnormalities, including swelling, fragmentation, a decreased count of cisternae within individual stack, and a rise in vesicles surrounding each stack. Notably, rTMS alleviated the above changes (Fig. 2H, I). These findings indicated that rTMS upregulated Dram1, and inhibited OGD/R-induced GA stress and neuronal damage.

Dram1 was transcriptionally activated by Gli2 in neurons

Next, we explored the reasons why Dram1 was upregulated by rTMS. In MCAO/R mice, Gli2 mRNA and protein levels were reduced, and this effect was reversed by rTMS (Figure S2A, B). Besides, Gli2 mRNA and protein levels were downregulated in OGD/R-induced primary neurons and N2a cells; however, this effect was progressively alleviated by increasing the rTMS intensity (Fig. 3A, B). Subsequently, sh-Gli2 was transfected into primary neurons and N2a cells to knockdown Gli2 expression (Fig. 3C, D). Moreover, Gli2 knockdown markedly reduced Dram1 mRNA and protein levels (Fig. 3E, F). Notably, the JASPAR database displayed the conserved DNA-binding motifs of Gli2 (Fig. 3G). Based on the prediction by JASPAR database, Gli2 and *Dram1* promoters have multiple binding sites. We screened the three sites with the highest binding scores for truncation experiments (sites 1-3). The dual-luciferase reporter gene vector containing the truncated sequences were named separately as Dram1-Luc1 (-2000 to

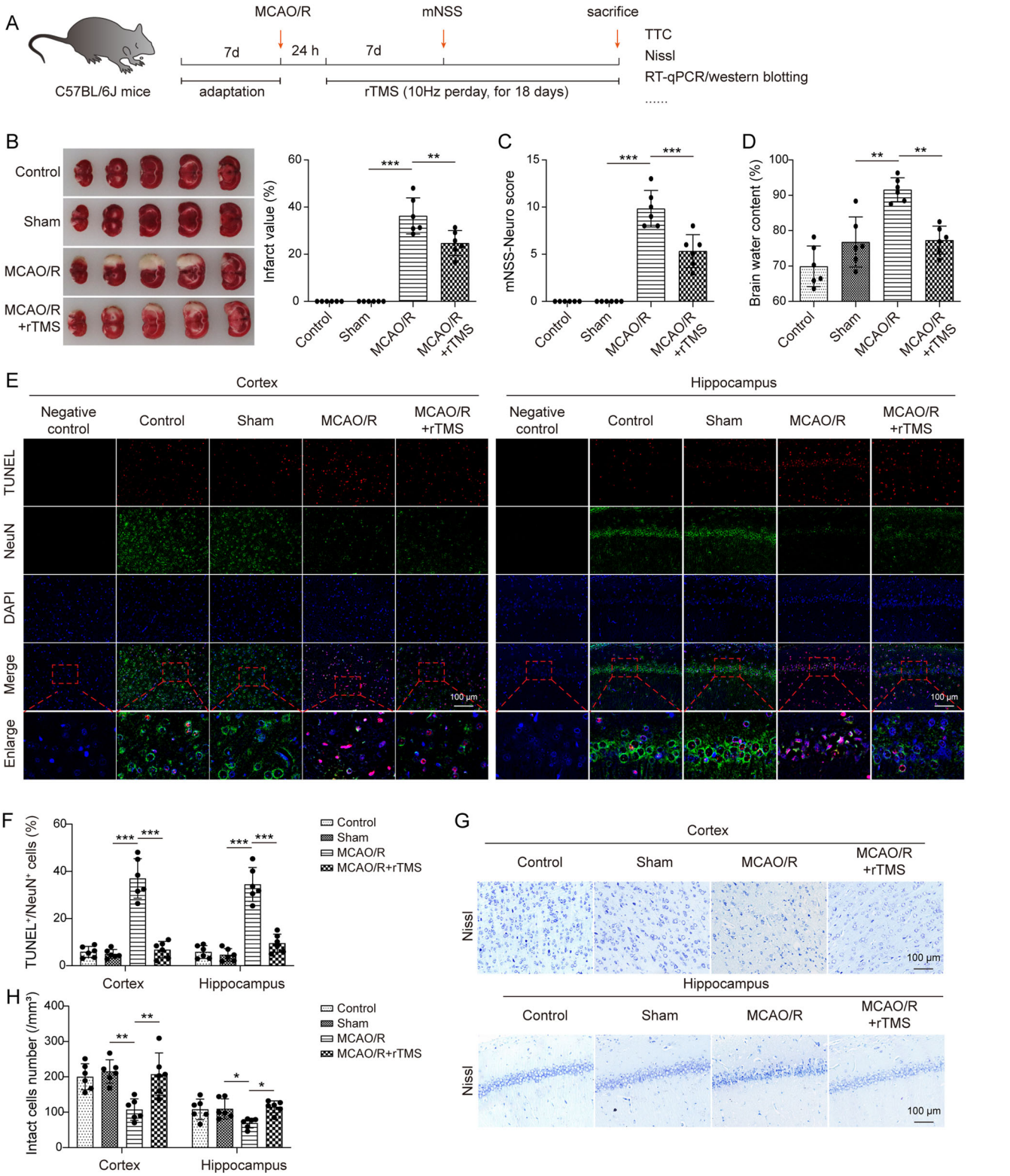

Fig. 1 | rTMS ameliorated brain injury in MCAO/R mice. C57BL/6 J mice were treated with MCAO/R surgery to induce cerebral I/R injury, followed by 10 Hz rTMS stimulation. **A** The flow chart of experiments with MCAO/R treatment and rTMS stimulation in mice. **B** TTC staining was performed to test the infarct area in mouse brain tissues at 18 days after rTMS treatment ($n = 6$). **C** Neurological function in mice at 7 days after rTMS treatment was assessed using mNSS ($n = 6$). **D** The water content of the mouse brain was determined using the wet/dry weight ratio method ($n = 6$). **E**, **F** Colocalization of NeuN and TUNEL in cortical and hippocampal regions of mouse brain tissues ($n = 6$). **G**, **H** Neurological damage in cortex and hippocampus was examined by Nissl's staining ($n = 6$). For (**B**–**H**), one-way ANOVA with Tukey's post hoc test was performed to analyze data. $^{*}P < 0.05$, $^{**}P < 0.01$ and $^{***}P < 0.001$.

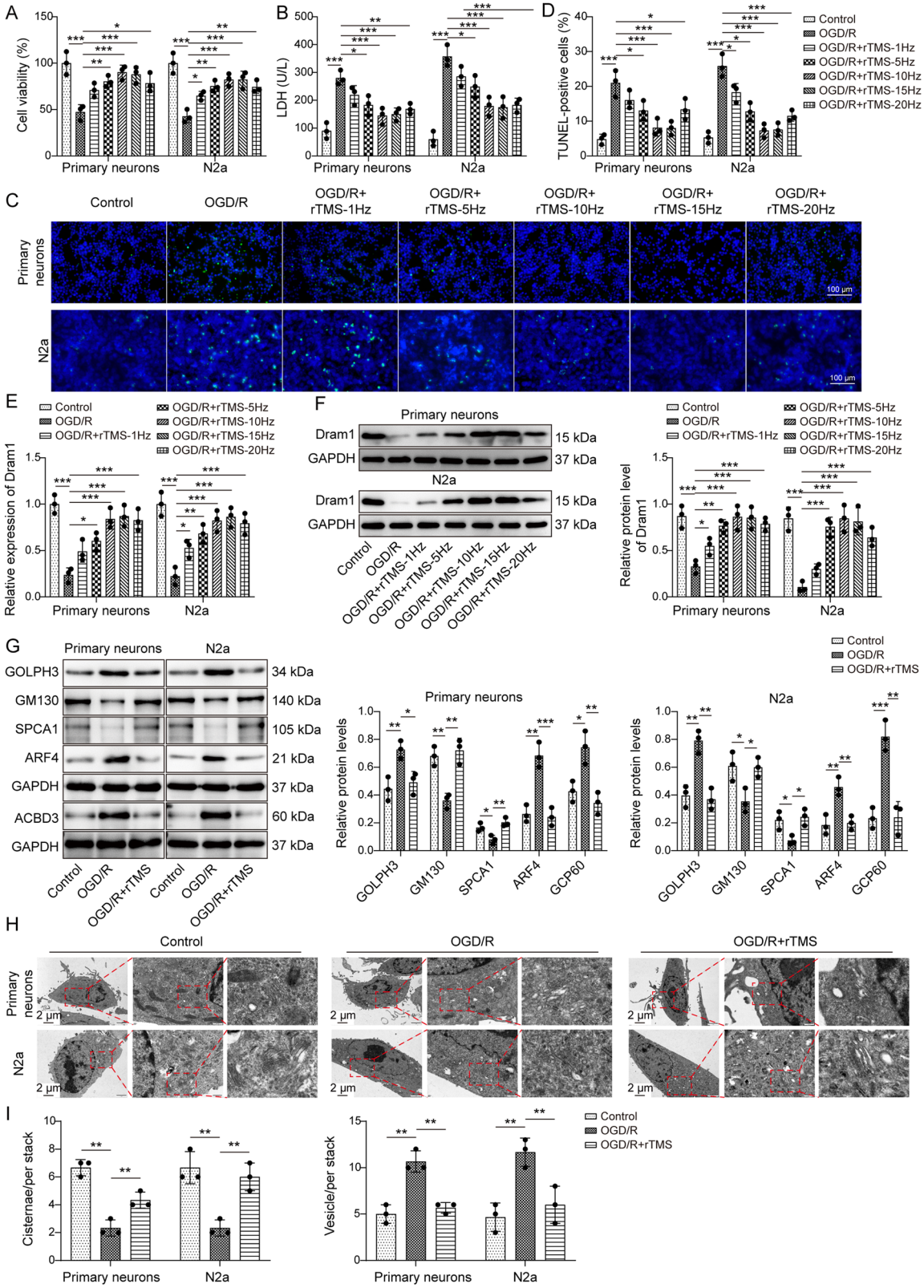

Fig. 2 | rTMS suppressed OGD/R-induced GA stress and neuronal damage by upregulating Dram1. Primary neurons and N2a cells were subjected to OGD/R treatment and treated with 1, 5, 10, 15 and 20 Hz rTMS, respectively. **A** CCK-8 assay was employed to measure cell viability. **B** LDH levels were tested in primary neurons and N2a cells by ELISA kit. **C**, **D** Apoptosis was evaluated by TUNEL staining. **E**, **F** Dram1 mRNA and protein levels were detected using RT-qPCR and western blotting, respectively. Based on the experimental results, the optimal rTMS frequency (10 Hz) was selected for subsequent experiments. **G** Levels of GA functional and structural proteins (GOLPH3, GM130, SPCA1, ARF4, and ACBD3) were measured by western blotting. **H**, **I** Morphology and ultrastructure of GA in primary neurons and N2a cells were detected using transmission electron microscopy and the numbers of cisternae and vesicle surrounding each stack were analyzed. $n = 3$. For **A**–**I**, one-way ANOVA with Tukey's post hoc test was performed to analyze data. $^{*}P < 0.05$, $^{**}P < 0.01$ and $^{***}P < 0.001$.

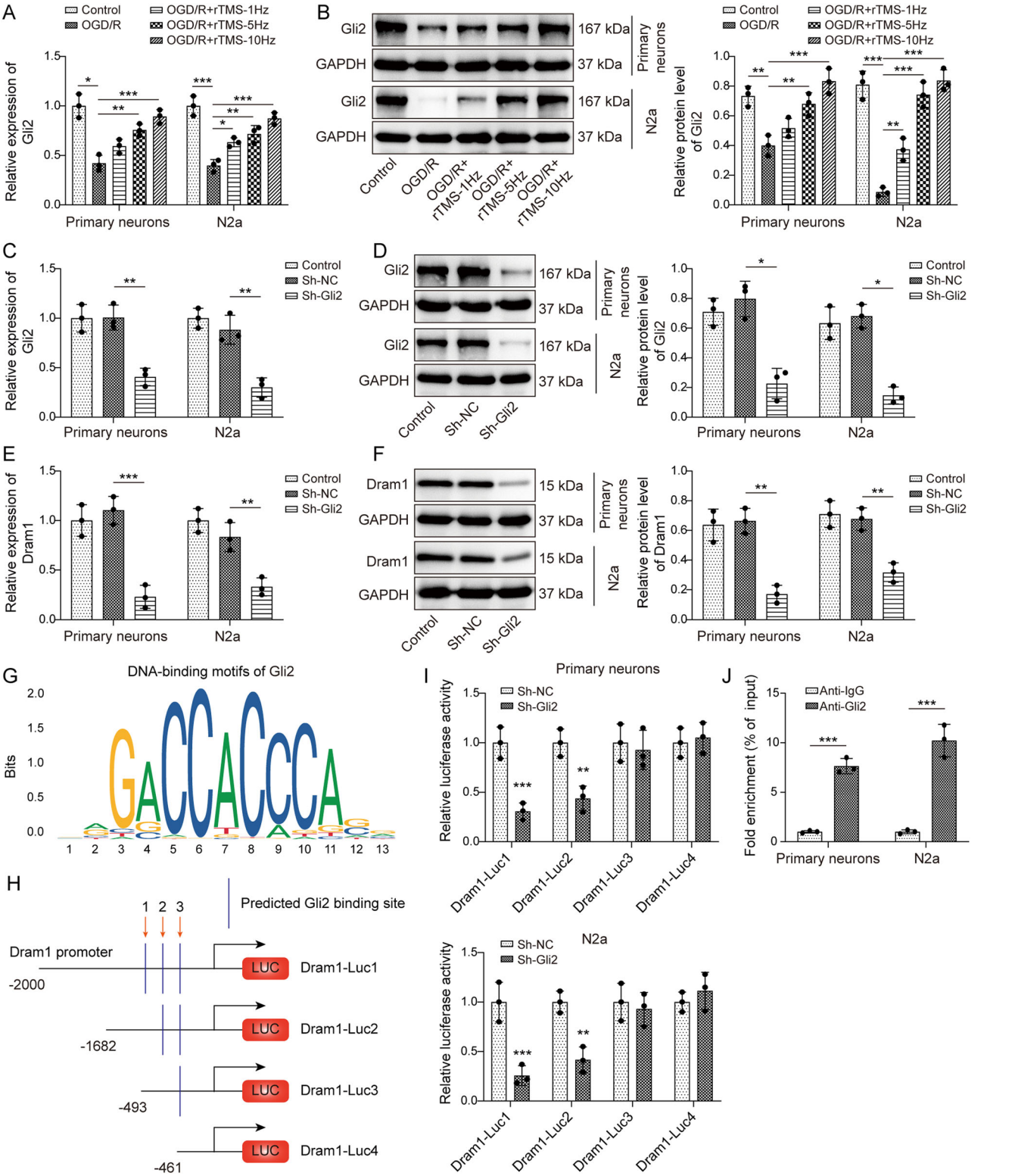

Fig. 3 | *Dram1* was transcriptionally activated by Gli2 in neurons. A, **B** Primary neurons and N2a cells were subjected to OGD/R treatment for 3 h, and then cells were stimulated using 1, 5, 10 Hz rTMS. Gli2 mRNA and protein levels were examined by RT-qPCR and western blotting. **C**–**F** sh-NC or sh-Gli2 was transfected into primary neurons and N2a cells, respectively, and the levels of Gli2 (**C**, **D**) and Dram1 (**E**, **F**) were examined by RT-qPCR and western blotting, respectively. **G** The conserved DNA-binding motifs of Gli2 were predicted by JASPAR database (https://jaspar.elixir.no/). **H** The truncated image of the Dram1 promoter region. **I** The relative luciferase activities of Dram1-Luc-1, Dram1-Luc-2, Dram1 Luc-3, and Dram1-Luc4 was tested by dual-luciferase reporter gene experiments in primary neurons and N2a cells after knockdown of Gli2. **J** The binding relationship of Gli2 to the Dram1 promoter was verified by ChIP. $n = 3$. One-way ANOVA with Tukey's post hoc test (for **A**–**F**) and Student's t test (for **I**, **J**) were performed to analyze data. $^{*}P < 0.05$, $^{**}P < 0.01$ and $^{***}P < 0.001$.

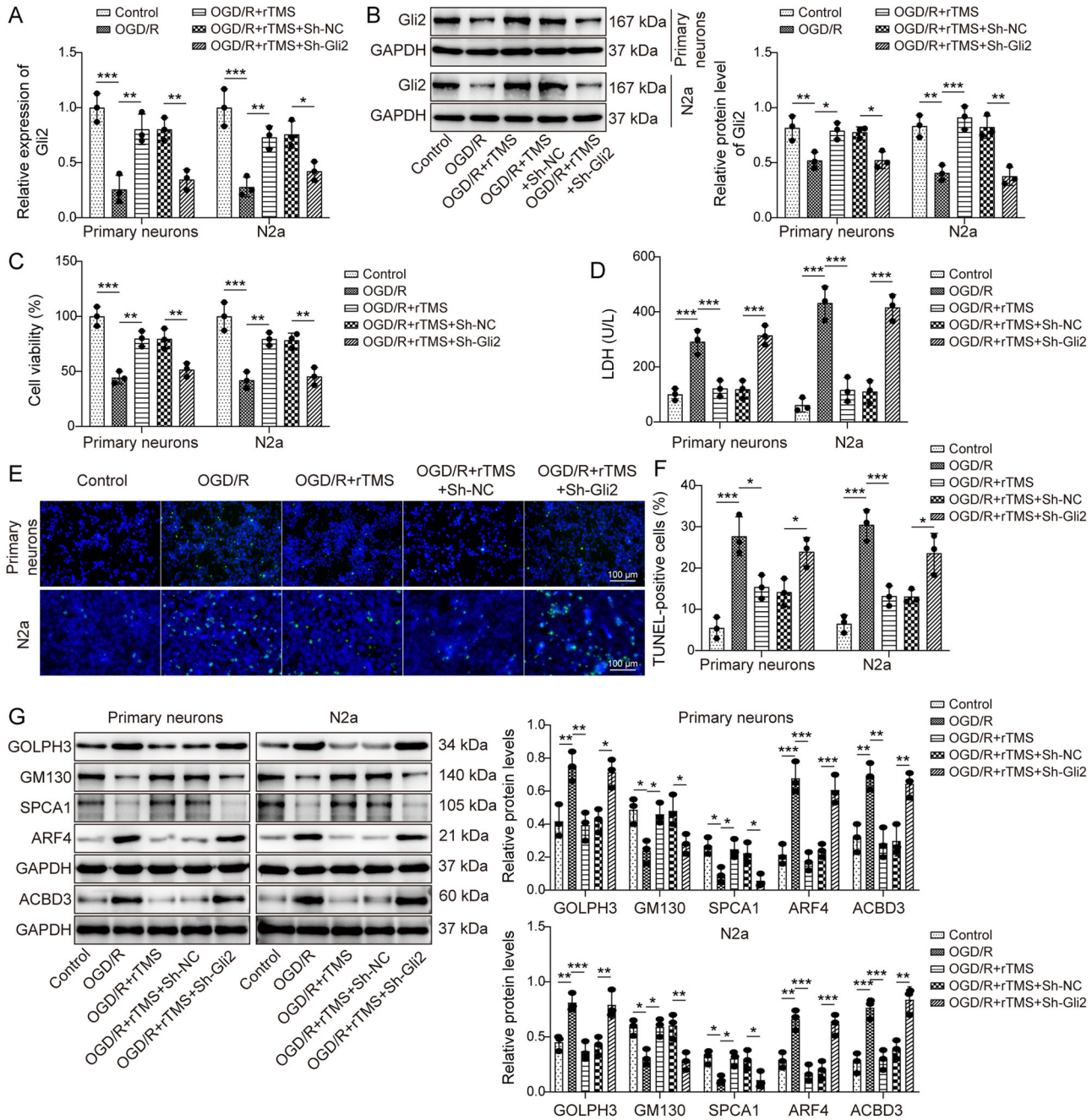

Fig. 4 | Knockdown of Gli2 reversed the effects of rTMS on OGD/R-induced GA stress and neuronal damage. The sh-NC or sh-Gli2 was transfected into primary neurons and N2a cells treated with OGD/R and rTMS, respectively. **A**, **B** RT-qPCR and western blotting assays were performed to determine the Gli2 levels in primary neurons and N2a cells. **C** Cell viability was assayed using a CCK-8 kit. **D** LDH levels in primary neurons and N2a cells were measured using ELISA kit. **E**, **F** Apoptosis was examined using the TUNEL assay. **G** The expression levels of GA functional and structural proteins (GOLPH3, GM130, SPCA1, ARF4, and ACBD3) were determined by western blotting. $n = 3$. One-way ANOVA with Tukey's post hoc test was performed to analyze data. $^{*}P < 0.05$, $^{**}P < 0.01$ and $^{***}P < 0.001$.

-461), Dram1-Luc2 (-1682 to -461), Dram1-Luc3 (-493 to -461) and Dram1-Luc4 (-461-0) (Fig. 3H). Subsequently, the above reporter vectors and sah-Gli2/sh-NC were co-transfected into primary neurons and N2a cells. Dual-luciferase reporter gene results showed that the relative luciferase activity of the Dram1-Luc1 group was significantly reduced after knockdown of Gli2; Dram1-Luc2 group also showed slightly reduced luciferase activity, but the relative luciferase activity was not significantly changed after transfection of Dram1-Luc3 and Dram1-Luc4 (Fig. 3I). The above results suggest that the first two sites were required for Gli2 to regulate Dram1 transcription. In addition, ChIP results revealed that Dram1 was enriched after immunoprecipitation with an anti-Gli2 antibody (Fig. 3J). These results suggested that Gli2 transcriptionally activated Dram1 in primary neurons and N2a cells.

rTMS alleviated OGD/R-induced GA stress and neuronal damage by increasing Gli2

Next, we explored whether Gli2 is involved in the process of rTMS improving neuronal GA stress and neuronal damage. We found that Gli2 levels were downregulated in OGD/R-induced primary neurons and N2a cells, which were upregulated by rTMS treatment, and Gli2 knockdown reversed the regulatory effect of rTMS (Fig. 4A, B). Furthermore, rTMS enhanced the OGD/R-induced neuronal cell viability, whereas Gli2

knockdown counteracted the effects of rTMS (Fig. 4C). Treatment with OGD/R increased LDH levels in neurons, whereas rTMS led to a decrease in LDH levels. Further knockdown of Gli2 reversed the action of rTMS (Fig. 4D). rTMS also inhibited OGD/R-induced neuronal apoptosis, which was abolished by Gli2 knockdown (Fig. 4E, F). In addition, OGD/R treatment significantly upregulated the protein levels of GOLPH3, ARF4, and ACBD3, and downregulated the levels of GM130 and SPCA1 (Fig. 4G). rTMS reversed the interference of OGD/R with these GA functional and structural proteins, and Gli2 knockdown restored their levels to those observed in OGD/R treatment (Fig. 4G). What's more, the expression level of Gli2 was significantly upregulated after oe-Gli2 transfection in primary neurons and N2a cells (Figure S3A, B). Under OGD/R condition, Gli2 levels were significantly reduced, rTMS reversed the effects of OGD/R, and further Gli2 overexpression enhanced the effects of rTMS (Figure S3C, D). In addition, Gli2 overexpression enhanced the promoting effect of rTMS on cell viability (Figure S3E) and further inhibiting LDH release (Figure S3F) and apoptosis (Figure S3G, H) in OGD/R-treated neurons. OGD/R treatment significantly upregulated GOLPH3, ARF4, and ACBD3 protein levels and downregulated GM130 and SPCA1 protein levels (Figure S3I). rTMS stimulation reversed the effects of OGD/R on the levels of these GA functional and structural proteins, and overexpression of Gli2 further enhanced the effects of rTMS (Figure S3I). It is evident that rTMS plays an essential role in alleviation of OGD/R-induced GA stress and neuronal damage by regulating Gli2.

rTMS promoted Gli2 expression by inhibiting HDAC5

The above findings suggest that rTMS affects the neuronal GA stress under I/R condition by upregulating Gli2. However, the regulatory mechanisms underlying the effects of rTMS and Gli2 remain unknown. It has been reported that rTMS could induce persistent changes in histone acetylation in mice[22]. However, it is not entirely clear whether rTMS is able to modulate Gli2 expression by altering the histone acetylation level of related enzymes, which ultimately affects neuronal function. In our study, rTMS treatment notably reduced HDAC5 protein expression in OGD/R-induced primary neurons and N2a cells but had no obvious impact on the expression of HDAC1, 2, 3, and 4 (Fig. 5A). Moreover, MCAO/R treatment in mice upregulated HDAC5 protein level, which was reversed by rTMS treatment (Figure S2C). Subsequently, oe-HDAC5 was transfected into primary neurons and N2a cells, and the results shown in Fig. 5B, C demonstrated the successful overexpression of HDAC5. Additionally, HDAC5 overexpression lowered the Gli2 mRNA and protein levels in primary neurons and N2a cells (Fig. 5D, E). Importantly, OGD/R treatment increased HDAC5 expression and suppressed Gli2 expression in primary neurons and N2a cells. However, after rTMS treatment, HDAC5 levels were downregulated and Gli2 levels were upregulated. Furthermore, HDAC5 overexpression counteracted the effects of rTMS treatment (Fig. 5F–H). Consequently, rTMS increased Gli2 expression in primary neurons and N2a cells by inhibiting HDAC5 expression.

HDAC5 inhibited H3K27ac modification of the *Gli2* promoter region in neurons

Considering the important role of HDAC5 in influencing gene transcription through histone deacetylation, ChIP experiments were conducted to examine H3K9ac, H3K14ac and H3K27ac enrichment in the *Gli2* promoter region. Our results indicated that OGD/R treatment reduced H3K9ac and H3K27ac enrichment in *Gli2* promoter region compared to that in control group, whereas rTMS increased the H3K27ac enrichment (Fig. 6A). However, treatment with OGD/R and rTMS had almost no effect on H3K14ac level (Fig. 6A). Our study revealed a binding relationship between HDAC5 and the *Gli2* promoter (Fig. 6B). Moreover, HDAC5 overexpression inhibited H3K27ac enrichment in *Gli2* promoter (Fig. 6C). We further treated primary neurons and N2a cells with LMK253, an HDAC5 inhibitor, which enhanced H3K27ac enrichment in *Gli2* promoter region (Fig. 6D). These results indicated that HDAC5 inhibited the modification of H3K27ac in *Gli2* promoter.

Overexpression of Dram1 reversed the effects of Gli2 knockdown on OGD/R-induced neuronal GA stress and damage under rTMS treatment

To further elucidate how Gli2 and Dram1 affect OGD/R-induced neuronal GA stress and damage following rTMS treatment, sh-Gli2 and oe-Dram1 were transfected into N2a cells. Our results indicated that Dram1 was successfully overexpressed in N2a cells by oe-Dram1 transfection (Fig. 7A, B). Notably, rTMS upregulated the level of Dram1 in OGD/R-treated cells, whereas Gli2 knockdown decreased the level of Dram1; further overexpression of Dram1 reversed the effect of Gli2 knockdown (Fig. 7C, D). Furthermore, Gli2 knockdown inhibited the enhancement of OGD/R cell viability induced by rTMS, whereas Dram1 overexpression restored N2a cell viability (Fig. 7E). Treatment with rTMS reduced LDH levels in OGD/R-treated cells; however, when Gli2 was suppressed, LDH levels were increased. However, Dram1 overexpression reversed the effects of knockdown of Gli2, leading to a decrease in LDH levels (Fig. 7F). Meanwhile, knockdown of Gli2 reversed the inhibitory effect of rTMS on apoptosis in OGD/R-treated cells, which was counteracted by further overexpression of Dram1 (Fig. 7G, H). In exploring the GA functional and structural proteins, rTMS treatment suppressed the expression of GOLPH3, ARF4, and ACBD3, and promoted the expression of GM130 and SPCA1 in OGD/R cells. However, Gli2 knockdown reversed the effects of rTMS, and overexpression of Dram1 reversed the impact of Gli2 knockdown (Fig. 7I). The above results indicated that rTMS ameliorated OGD/R-induced neuronal GA stress and damage by promoting the Gli2/Dram1 axis.

Gli2 knockdown reversed the effects of rTMS in ameliorating the GA stress and brain injury in MCAO/R mice

Finally, we further verified the effect of Gli2 on rTMS-treated MCAO/R mice. A flowchart of the experiment was shown in Fig. 8A: C57BL/6 J mice were subjected to MCAO/R treatment and Gli2 knockdown after one week of adaptive feeding, followed by 10 Hz rTMS treatment for 18 days. Our results demonstrated that Gli2 inhibition reversed the mitigating effect of rTMS on cerebral infarction in MCAO/R mice (Fig. 8B). rTMS attenuated MCAO/R-induced neurological deficits, and Gli2 knockdown reversed these effects (Fig. 8C). rTMS reduced the increase in brain water content caused by MCAO/R, but knockdown of Gli2 reversed the effects of rTMS (Fig. 8D). Furthermore, Gli2 knockdown reversed the ameliorative effect of rTMS on neuronal injury in cortex and hippocampus of MCAO/R mice (Fig. 8E, F). Additionally, rTMS stimulation reversed the downregulation of Gli2 and Dram1 induced by MCAO/R treatment, and knockdown of Gli2 reversed the effects of rTMS (Fig. 8G). Importantly, Gli2 knockdown reversed the protective effect of rTMS on GA stress (Fig. 8H). Thus, our results demonstrated that Gli2 knockdown reversed the ameliorative effects of rTMS on the GA stress and brain injury in MCAO/R mice.

Discussion

Cerebral ischemic stroke is the second leading cause of death in humans, and its incidence increases every year[32]. Restoration of blood flow and oxygenation is key to treating cerebral ischemic diseases; however, the process of I/R generates large amounts of reactive oxygen species (ROS) and oxygen free radicals, resulting in neurological dysfunction and affecting patient prognosis[33]. Numerous studies have demonstrated that rTMS is a promising therapy for cerebral ischemic stroke because it modulates cortical excitability and increases neuronal plasticity[34]. Clinical studies have revealed that rTMS improves multiple neurological deficits such as speech, cognition, and motor function in patients with cerebral ischemic stroke[35]. At the animal level, rTMS reduces the area of cerebral infarction in MCAO/R mice[35]. However, the exact underlying mechanism remains unclear. Here, we found that rTMS reduced the area of cerebral infarction, degree of cerebral edema, and neurological damage in MCAO/R mice model, and effectively inhibited OGD/R-induced neuronal injury and GA stress in vitro. Mechanistically, rTMS promoted the transcriptional activity of *Dram1* by attenuating the inhibitory effect of HDAC5 on H3K27ac modification of *Gli2* promoter.

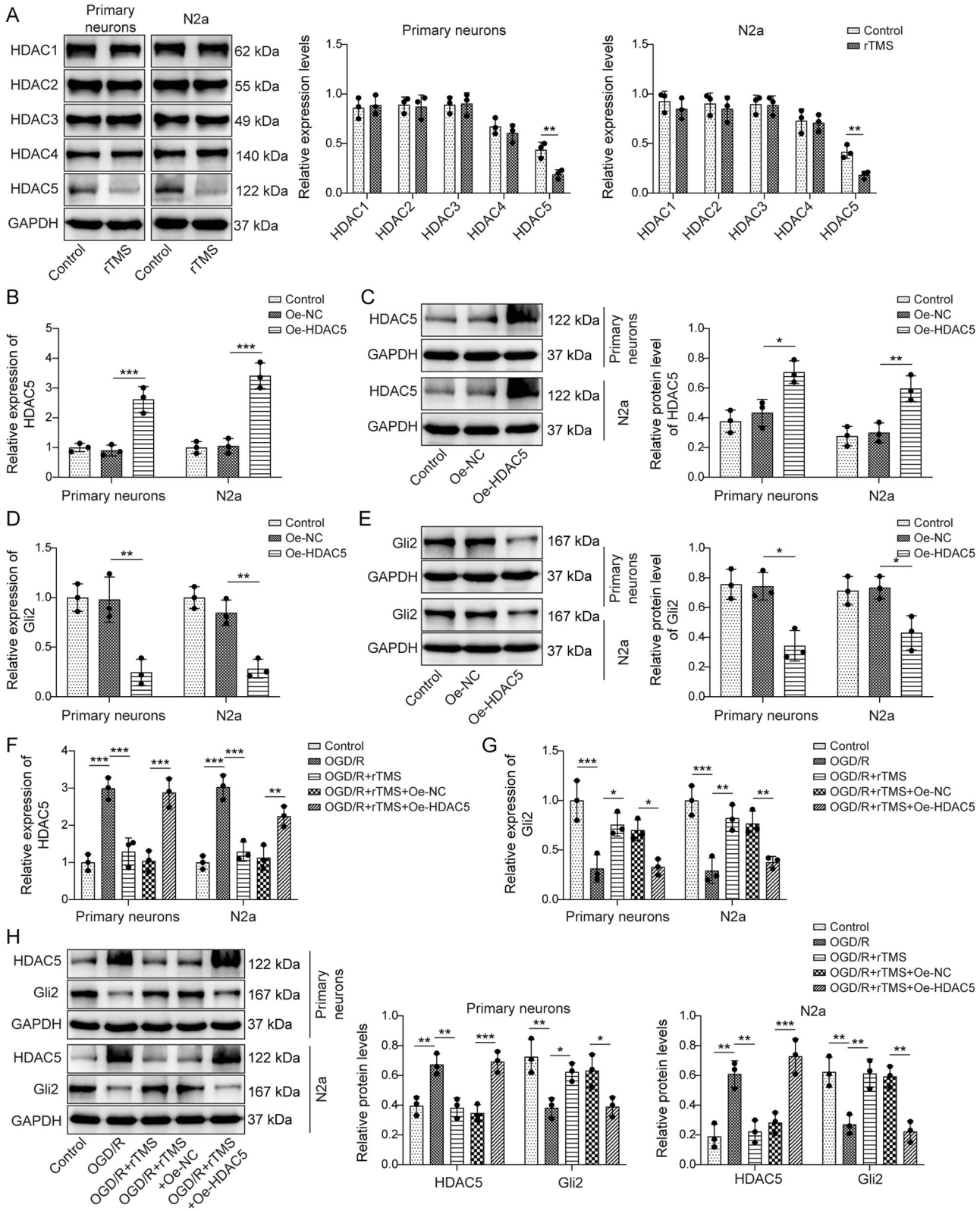

Fig. 5 | rTMS promoted Gli2 expression by inhibiting HDAC5. A HDAC1-5 expression levels in rTMS-treated primary neurons and N2a cells were checked by western blotting. **B**, **C** The effect of HDAC5 overexpression was detected by RT-qPCR and western blotting in primary neurons and N2a cells. **D**, **E** RT-qPCR and western blotting were applied to check the influence of HDAC5 overexpression on Gli2 mRNA and protein levels. **F**–**H** HDAC5 overexpression vector or its negative control oe-NC was transfected into primary neurons and N2a cells with OGD/R and rTMS treatments, and mRNA (**F, G**) and protein (**H**) levels of HDAC5 and Gli2 were detected using RT-qPCR and western blotting. $n = 3$. Student's t test (for **A**) and one-way ANOVA with Tukey's post hoc test (for **B**–**H**) were performed to analyze data. $^{*}P < 0.05$, $^{**}P < 0.01$ and $^{***}P < 0.001$.

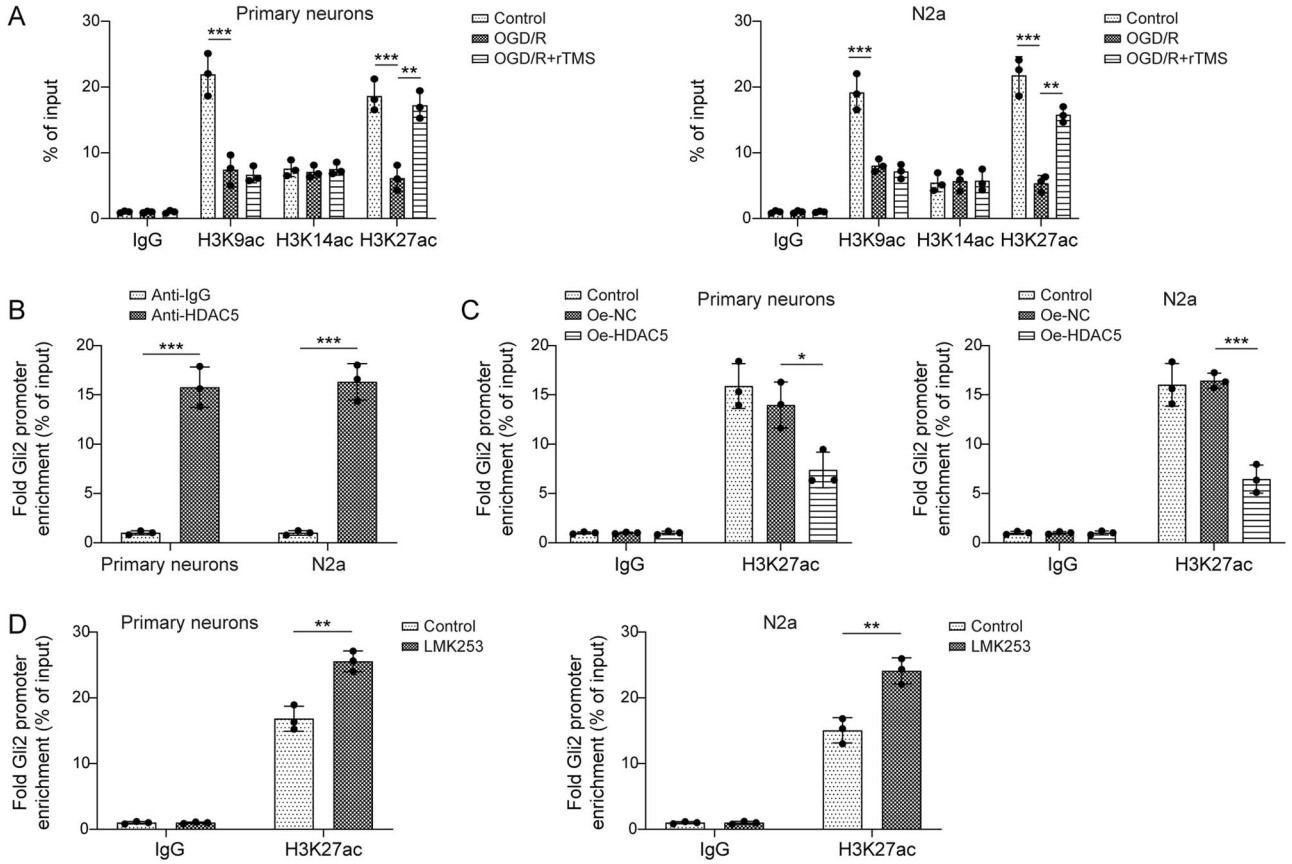

Fig. 6 | HDAC5 inhibited H3K27ac modification of the *Gli2* promoter region in neurons. A Primary neurons and N2a cells were treated with OGD/R and 10 Hz rTMS. H3K9ac, H3K14ac, and H3K27ac enrichment in *Gli2* promoter region was detected by ChIP assay. **B** ChIP was performed to assay the binding relationship between HDAC5 and *Gli2* promoter in primary neurons and N2a cells. **C** The effect of overexpression of HDAC5 on H3K27ac enrichment in *Gli2* promoter region was tested by ChIP assay. **D** H3K27ac enrichment in *Gli2* promoter region was measured by ChIP after treatment of primary neurons and N2a cells with an inhibitor of HDAC5 (LMK253). $n = 3$. One-way ANOVA with Tukey's post hoc test (for **A** and **C**) and student's t test (for **B**, **D**) were performed to analyze data. $^{*}P < 0.05$, $^{**}P < 0.01$ and $^{***}P < 0.001$.

GA is a sensor and downstream effector of stress in cell death pathways[9]. Under stress, GA structure and function are disrupted, causing an alteration in the redox balance of cells and an increase in cell mortality[36]. Extensive research has indicated the strong association between GA stress and neurodegenerative diseases, including cerebral ischemic stroke[5,37]. For instance, UBIAD1 reduces neuronal death by restoring mitochondrial and GA damage during cerebral I/R injury[5]. The highly dynamic and unique structure of GA relies on structural GA proteins that act as scaffolds or matrices to support the morphology and function of GA[38]. During oxidative stress, downregulation of the GA structure-associated protein GM130 leads to the fragmentation of GA and the impaired GA function, ultimately triggering apoptosis[39]. Li et al.[40] reported that GM130 impeded OGD/R-induced GA division and apoptosis. SPCA1 is mainly responsible for maintaining correct GA structure[7]. Previous studies reported the upregulated SPCA1 expression attenuated GA swelling, and inhibited neuron lyse in in vitro and in vivo models of cerebral ischemic stroke[10]. GOLPH3 is a sensor of GA stress that rapidly increases during oxidative stress, transmitting downstream stress signals and inducing ROS production in cells, thereby promoting GA disintegration[39]. He et al.[7] found that GOLPH3 was upregulated and GA was fragmented in OGD/R and MCAO/R mice. ACBD3 is a GA stress protein, and downregulation of ACBD3 often indicates that the GA stress is inhibited[41]. Up-regulation of the COOH-terminal structural domain of ACBD3 resulted in GA structural breakdown and inhibited protein translocation from endoplasmic reticulum to GA[42]. ARF4 is a signal transduction molecule in the GA membranes. When its expression was reduced, it directly inhibited GA stress and restored the inhibitory morphological differentiation phenotype[43]. In the present study, we observed structural edema and fragmentation of GA, upregulation of GOLPH3, ARF4, and ACBD3, and downregulation of GM130 and SPCA1 in MCAO/R mice and OGD/R-treated cells, suggesting that cerebral ischemia activated GA stress and led to destruction of GA structure and function. Moreover, we demonstrated that rTMS alleviated the neuronal GA stress induced by cerebral ischemic stroke in vivo and ameliorated neuronal OGD/R injury in vitro.

Dram1 is an important factor that regulates stress response in GA. Dram1 deficiency affects the organization and function of GA[30]. A previous study revealed that Dram1 inhibited abnormally shaped GA, improving neuronal defects in mice[44]. A previous study suggested that Dram1 knockdown exacerbated OGD/R-induced cellular damage[29]. In the present study, Dram1 expression was reduced in brain tissues of MCAO/R-induced mice and OGD/R-induced neurons. We revealed that rTMS suppressed cerebral I/R-induced GA stress and neuronal damage by upregulating Dram1. Therefore, Dram1 may be a key regulator of GA stress in neurons modulated by rTMS.

Gli2 is a transcription factor that activates the transcription of target genes. Gli2 is important for the regulation of miRNA target genes associated with spinal cord I/R injury[45]. Importantly, it was shown that Gli2 alleviated cerebral I/R injury by promoting the transcription of *lncRNA Peg13*[25]. We demonstrated that *Dram1* was transcriptionally activated by Gli2 in neurons. Gli2 expression has recently been shown to be reduced in OGD/R cells, and Gli2 overexpression relieves I/R-induced cerebral edema, cerebral infarction, and neurological deficits[25]. In the present study, Gli2 expression was reduced, whereas rTMS treatment increased Gli2 expression in MCAO/R mice. Moreover, Gli2 knockdown impaired the protective role of rTMS against OGD/R-induced GA stress and neuronal damage. Dram1

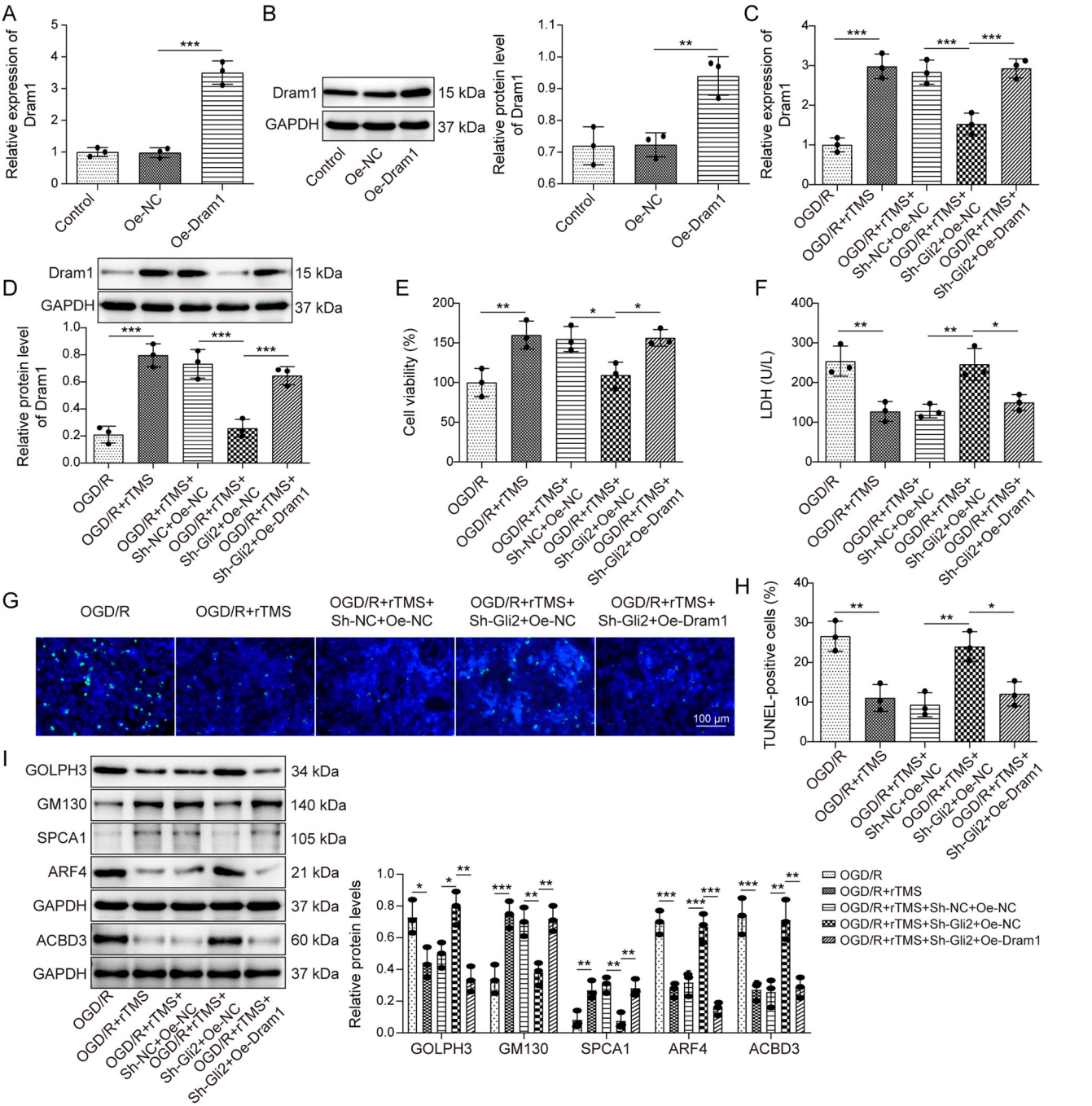

Fig. 7 | Overexpression of Dram1 reversed the effects of Gli2 knockdown on OGD/R-induced neuronal GA stress and damage under rTMS treatment. A, B After Dram1 overexpression vector or its negative control oe-NC was transfected into N2a cells, Dram1 levels were tested by RT-qPCR and western blotting. sh-Gli2, Dram1 overexpression vector, and their negative controls were transfected into N2a cells, which were then subjected to OGD/R and 10 Hz rTMS treatment. **C, D** RT-qPCR and western blotting were applied to analyze the expression levels of Dram1. **E** Cell viability was determined by the CCK-8 assay. **F** LDH levels were tested using ELISA kit. **G, H** Apoptosis was assessed by TUNEL staining. **I** Levels of GOLPH3, GM130, SPCA1, ARF4, and ACBD3 were assayed using western blotting. $n = 3$. One-way ANOVA with Tukey's post hoc test was performed to analyze data. $^{*}P < 0.05$, $^{**}P < 0.01$ and $^{***}P < 0.001$.

overexpression reversed the effects of Gli2 knockdown. Therefore, rTMS treatment ameliorated cerebral I/R injury by promoting Gli2 transcriptional activation of *Dram1*.

Previous studies in the literature indicated that rTMS induced persistent changes in histone acetylation of related factors in mice[22] and HDACs happened to be the histone deacetylases that regulated protein acetylation and chromatin remodeling[46]. Furthermore, the inhibition of some allosteric forms of HDACs reportedly protects the cerebrum from ischemic injury. HDAC5 is a class II HDACs widely expressed in MCAO/R mice and OGD/R-treated cells[21]. The inhibition of HDAC5 impedes the death of nerve cells, preventing cerebral I/R damage[47]. In the present study, HDAC5 was significantly upregulated in OGD/R-treated neurons, whereas rTMS treatment suppressed HDAC5 expression. Notably, Wang et al.[48] reported that HDAC5 knockdown alleviated spinal cord injury-induced pain in central nervous system by increasing H3K27ac enrichment in *NEDD4* promoter. In our study, OGD/R treatment suppressed H3K27ac enrichment in *Gli2* promoter region, whereas rTMS treatment led to an increase in H3K27ac enrichment. Furthermore, the overexpression of HDAC5 counteracted the

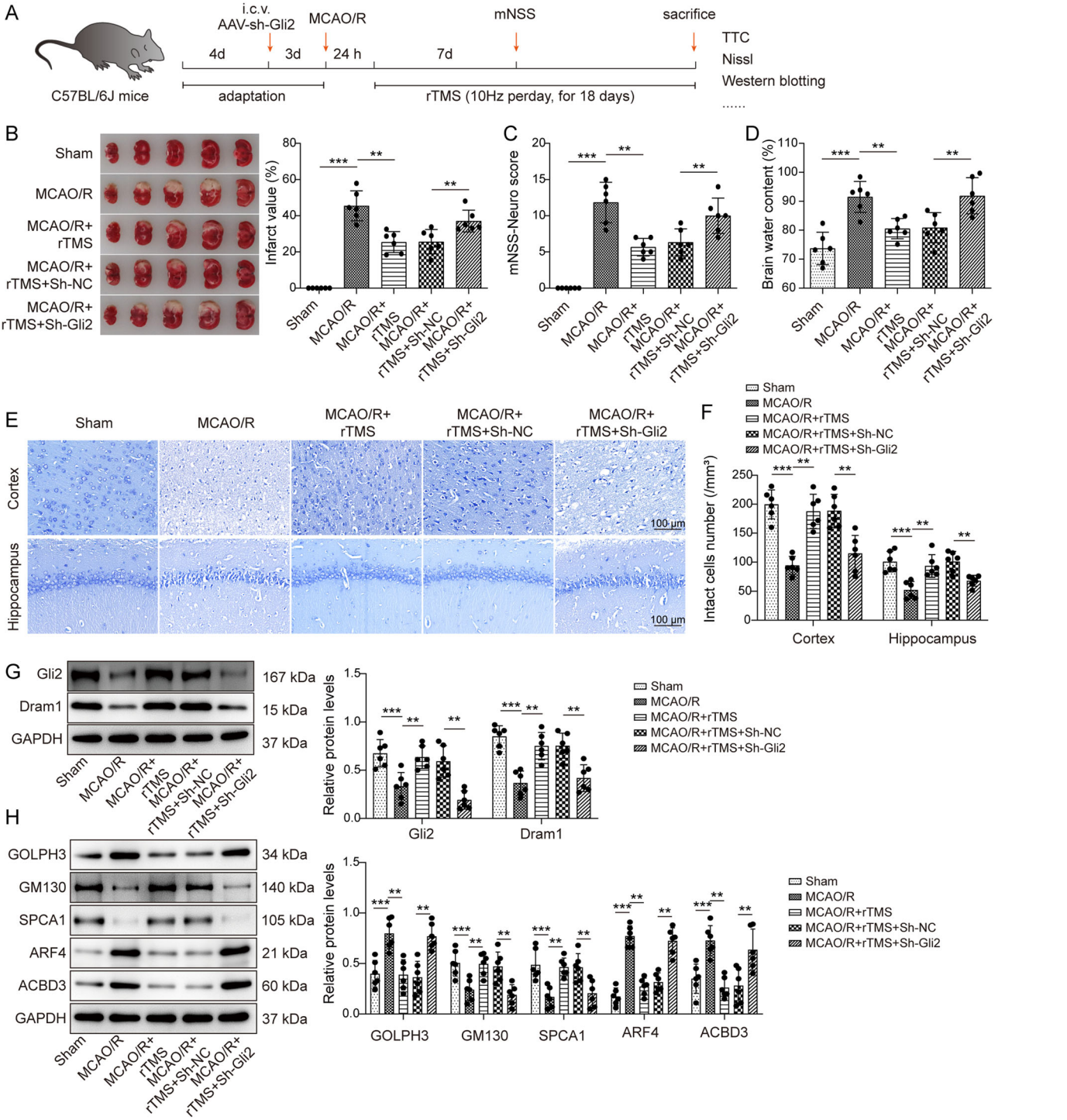

Fig. 8 | Knockdown of Gli2 reversed the effects of rTMS in ameliorating GA stress and brain injury in MCAO/R mice. The sh-Gli2 or sh-NC adenovirus was injected into the lateral ventricle of MCAO/R mice, which were then treated with 10 Hz rTMS. **A** The flow chart of the rTMS and adenovirus treatment to C57BL/6 J mice. **B** TTC staining was performed to test the infarct area in the mouse brain tissues at 18 days after rTMS treatment ($n = 6$). **C** Neurological function in mice was assessed using mNSS at 7 days after rTMS treatment ($n = 6$). **D** The water content of the mouse brain was determined using the wet/dry weight ratio method ($n = 6$). **E**, **F** Nissl staining was used to measure nerve damage in mice ($n = 6$). **G** The protein levels of Gli2 and Dram1 in brain tissues were determined by western blotting assays ($n = 6$). **H** The protein levels of GA functional and structural proteins (GOLPH3, GM130, SPCA1, ARF4, and ACBD3) in brain tissues were measured using western blotting ($n = 6$). One-way ANOVA with Tukey's post hoc test was performed to analyze data. $^{*}P < 0.05$, $^{**}P < 0.01$ and $^{***}P < 0.001$.

effects of rTMS. Thus, rTMS alleviated OGD/R-induced GA stress and neuronal damage by inhibiting HDAC5 to increase H3K27ac modification in *Gli2* promoter region.

In summary, this study indicates that rTMS can ameliorate cerebral I/R injury by reducing GA stress. The mechanism is that rTMS inhibits the histone deacetylation of *Gli2* promoter region by suppressing HDAC5, and the upregulated Gli2 facilitates the transcriptional activation of *Dram1*. Therefore, regulating GA stress may be a viable strategy for rTMS to mitigate cerebral I/R injury, and Gli2 and Dram1 may be key proteins in controlling GA stress. However, our study primarily focused on the effects of

rTMS on neuronal GA stress, and its role in other neuronal functions such as pyroptosis, autophagy, and necrosis requires further investigation.

Methods

Animals

A total of 221 adult male C57BL/6 J mice (SPF grade) aged 10 weeks were purchased from Hunan SJA Laboratory Animal Co., Ltd [SCXK (Xiang) 2019-0004]. C57BL/6 J mice were housed under alternating light and dark conditions for 12 h at 24.0 ± 2.0 °C and 50-60% relative humidity. All animal experiments were approved by the Ethics Committee and the Animal Care and Use Committee of Xiangya Second Hospital in accordance with the relevant guidelines (No. 20240144).

MCAO/R surgery

Two sets of animal experiments were performed, the first experimental set consisted of 4 groups: control, sham, MCAO/R, and MCAO/R+rTMS. The second experimental set comprised 5 groups: sham, MCAO/R, MCAO/R +rTMS+sh-NC, and MCAO/R+rTMS+sh-Gli2. A priori power analysis was performed using G*Power software to estimate the sample size required to yield 80% power to detect a significant ($P < 0.05$) effect of the treatment. Each group was randomly assigned 6 mice and all personnel involved in group assignment, experimentation, and data analysis were mutually blinded throughout the study. The MCAO/R model was established to simulate cerebral I/R injury. The mice were fixed on a heating pad with medical tape. Subsequently, the mice were anesthetized via intraperitoneal administration of 1% sodium pentobarbital (100 $mg{\cdot}kg^{-1}$). The depilated site of the mouse neck was disinfected using 75% alcohol, and an incision of approximately 3–4 cm in length was made vertically in the neck to isolate the external carotid artery (ECA), internal carotid artery (ICA), and left common carotid artery (LCCA). A microarterial clip was temporarily applied to achieve ICA and LCCA clamping. After distal ligation and incision of the ECA, the silicon-coated monofilament (diameter: 0.18 ± 0.01 mm) was slowly inserted from the ECA into the ICA to block blood flow from the middle cerebral artery for 60 min. The silicon-coated monofilament was then removed to achieve reperfusion. The skin incisions were sutured and sterilized. After the surgical procedure, the mice were relocated to a 28 °C incubator until they woke up. Subsequently, they were transferred to feeding cages under normal feeding condition. All mice were subjected to MCAO/R surgery, except those in the control and sham groups. Five mice died during the experiments and were subsequently excluded.

After last rTMS stimulation, the mice were anesthetized by intraperitoneal injection of sodium pentobarbital and sacrificed by spinal dislocation. The mice were divided into four cohorts, designated for 2,3,5-Triphenyl tetrazolium chloride (TTC) staining, brain water content measurement, pathological examinations (immunofluorescence, TUNEL, Nissl staining, and transmission electron microscopy), and biochemical assays (RT-qPCR and western blotting analysis).

Mouse neurological function score (mNSS)

Neurobehavioral testing was performed on all mice seven days after the MCAO/R model was constructed. Twenty-four hours before the test or training, mice were placed in a test chamber to adapt to their environment. mNSS was applied to detect neurological deficits in mice[49]. Mice were subjected to exercise (tail lift test and straight walking test), sensation (muscle test and balance beam test), and reflex tests (auricular reflex, corneal reflex, startle reflex, and muscle spasm). Mice that failed to complete these tests received the corresponding scores. The higher the mNSS, the more severe the nerve damage in mice.

TTC staining

The brain tissues were removed, washed with pre-cooled phosphate buffered saline (PBS), and rapidly frozen (−20 °C) for 30 min. Next, the brain tissues were made into 2 mm-thick sections and stained in TTC solution while being immersed in normal saline at 37 °C for 30 min in the dark. Brain slices were immersed in 4% paraformaldehyde for 24 h. After taking photographs, the infarct area of each slice was assessed using ImageJ software (GE Healthcare, Sunnyvale, CA, USA).

Determination of cerebral edema in mice using the wet/dry weight ratio

After the fresh brain tissues were washed with pre-cooled PBS, the medulla was removed. The water and blood on the surface of the brain tissues were then sucked with a qualitative filter paper. Subsequently, the left and right hemispheres were divided along distinctive longitudinal fissures of the brain. The weights of the two hemispheres were then weighed separately, which was the wet weight. The brain tissues were exposed to a constant temperature oven at 65 °C for 24 h, and its weight was determined to be the dry weight. Brain water content (%)=[(wet weight-dry weight)/wet weight]×100.

Nissl staining

Paraffin sections (4 μm) were sequentially immersed in xylene, ethanol (100%, 95%, 80%, and 70%), and distilled water for 3 min each. Subsequently, the slices were stained with 1% tar violet for 10 min and quickly rinsed with distilled water. The slices were separated using 70% alcohol for 30 s. The slices were soaked in ethanol (70%, 80%, 95%, and 100%) and xylene. Finally, sections were sealed and observed under an inverted microscope (Olympus, Tokyo, Japan). Five random fields were selected for each slice. Intact neurons (with clear cell bodies and nuclei) were counted, for the number of complete intact neurons decreases under the condition of neuron injury.

Cell culture

Brain tissues were extracted from newborn C57BL/6 J suckling mice within 48 h and washed in a dish with pre-cooled PBS. The meninges and blood vessels were carefully removed to isolate bilateral hippocampal tissues[50]. The tissues were chopped into small pieces, washed with PBS, and digested with 0.25% trypsin for 20 min. According to the ratio of "100 mL of serum per milliliter of trypsin", the serum was added to the digestive juices to stop digestion. The cell suspension was centrifuged and the supernatant was discarded. DMEM (Invitrogen, Carlsbad, CA, USA) containing 10% fetal bovine serum was added to the cell pellet, thoroughly mixed, and sieved. The cell suspension was then inoculated onto a culture plate containing polylysine and cultured in a constant-temperature incubator. After 6 h, the cell culture medium was changed to Neurobasal-A medium (Thermo Fisher Scientific) containing 1% L-glutamic acid and 1% penicillin. Primary neurons from the third passage were used in subsequent experiments. Neuro-2a (N2a) cells were obtained from the Cell Storage Center of the Chinese Academy of Sciences (Shanghai, China). The N2a cells were authenticated by short tandem repeats (STR) and were confirmed to be free of mycoplasma contamination. N2a cells were cultured in DMEM supplemented with 10% fetal bovine serum in a 37 °C incubator with 5% CO_2.

OGD/R induction

An in vitro model of cerebral I/R injury was established using OGD/R treatment. The culture medium of primary neurons and N2a cells were replaced with sugar-free and serum-free medium, treated at 37 °C and 1% O_2 for 6 h, then changed to complete medium, and cultured at 37 °C and 21% O_2 for 6 h[51].

rTMS treatment

For rTMS treatment, at 1 week prior to MCAO/R treatment, the mice were placed in a plastic cylinder containing noise for 1 h per day. After 24 h of MCAO/R treatment, the mice were fixed in a circular plastic cylinder that could be penetrated by magnetic fields. A magnetic stimulator (CCY-II, Wuhan, China) was used for the treatment. The parameters used were as follows: coil frequency at 10 Hz for 10 min/day and continuous stimulation performed for 18 days. The mice in the sham group were not subjected to magnetic stimulation.

For primary neurons and N2a cells, rTMS stimulation was performed after OGD/R treatment, and subsequent tests were performed at 3 h after stimulation. Briefly, the magnetic coil was placed 1 cm from the petri dish. Magnetic stimulation parameters were as follows: coil frequency of 1/5/10/15/20 Hz, 10 min/day, continuous stimulation for two days[51].

Plasmid transfection

Small interfering RNAs (shRNAs) against Gli2 (sh-Gli2) and its negative control (sh-NC) were synthesized by GenePharma (Shanghai, China). Full-length Gli2, HDAC5, or Dram1 genes and negative sequences were cloned into the pcDNA3.1$^{(+)}$ vector (Thermo Fisher Scientific) to construct overexpression plasmids for Gli2, HDAC5 or Dram1 (oe-Gli2, oe-HDAC5, and oe-Dram1) and their negative controls (oe-NC). Plasmids were transfected into primary neurons and N2a cells for 48 h using Lipofectamine 3000 (Thermo Fisher Scientific).

For animal experiments, sh-Gli2 or sh-NC adenoviruses were obtained from GenePharma (Shanghai, China). 72 h before MCAO/R surgery, sh-Gli2 or sh-NC adenoviruses (2×10^8 TU/mL) was injected into the ipsilateral ventricle (i.c.v, 3.5 mm in depth, 1.5 mm lateral, and 1 mm posterior from bregma).

Ultrastructure of GA

Cells and fresh brain tissues were prefixed in 2.5% glutaraldehyde phosphate buffer for 24 h, followed by 1% osmic acid buffer for 1 h. The samples were then dehydrated in layers using 50%, 70%, 90%, and 100% acetone. The epoxy mixture was then added to the samples. After 24 h, the samples were embedded in Epon 812 embedding agent (Sigma-Aldrich). Embedded blocks were cut into ultrathin sections of 70 nm thickness using a micro-slicer (Leica, Germany). Sections were sequentially stained with sodium acetate and lead citrate. Finally, the morphology of the GA was viewed using a transmission electron microscope (Hitachi, Tokyo, Japan) and photographed.

CCK-8 assay

The CCK-8 test kit was purchased from Shanghai Sangon Bioengineering Co., Ltd (E606335, China). The treated cells were seeded into 96-well plates (5000 cells/well) and then incubated with 10 μL of CCK-8 solution at 37 °C for 30 min. The absorbance of the solution was measured at 450 nm by using a TECAN Infinite M200 spectrophotometer (Tecan, Switzerland).

ELISA assay

The experiment was performed according to the instructions of the mouse lactate dehydrogenase (LDH) ELISA kit (MM-43732M2, Enzyme Immunization, Jiangsu, China), and the OD value at 450 nm was measured using a TECAN Infinite M200 (Tecan). Standard curves were plotted using Origin software (OriginLab, Northampton, MA, USA), and LDH levels were calculated for each group.

TUNEL staining

The experiments were conducted according to the guidelines of the TUNEL Apoptosis Detection Kit (Beyotime, Nanjing, China), using 4% paraformaldehyde to fix the cells. Nuclei were counterstained with 4', 6-diamidino-2-phenylindole (DAPI). The cells were then observed under a confocal microscope (Leica) and the percentage of apoptotic cells was calculated according to the ratio of the number of TUNEL-positive nuclei to the number of DAPI-stained nuclei.

Fresh brain tissues were fixed in 4% paraformaldehyde for 24 h. They were then embedded in paraffin and sectioned (4 μm thick). After dewaxing and hydrating the sections, a 3% hydrogen peroxide solution was added. The samples were incubated for 20 min at room temperature. Subsequent staining steps were the same as those used to stain the cells.

Immunofluorescence staining

The paraffin sections of the brain tissues were placed in 0.1 mol/L citric acid repair solution and heated in a microwave oven. Brain tissues were transferred to 0.2% Triton X-100 for 15 min and blocked with 10% goat serum for 1 h. Sections were incubated with anti-NeuN antibody (ab177487, 1:300, Abcam, Cambridge, MA, USA) and anti-GOLPH3 antibody (ab98023, 1:100, Abcam) overnight at 4 °C and then incubated with secondary antibody for 1 h. DAPI was added to the sections, which were then incubated for 15 min in the dark. Images were obtained using a fluorescence microscope (Leica).

Chromatin immunoprecipitation (ChIP) detection

ChIP experiments were performed using the EZ-ChIP kit (17-371, Millipore, Billerica, MA, USA) according to the manufacturer's instructions. The cells were soaked in 1% formaldehyde solution and then evenly mixed with glycine (2.5 M) to halt crosslinking. After rinsing with PBS, the cells were scraped, collected, centrifuged, and precipitates were obtained. These precipitates were resuspended, and after addition of the protease inhibitor mixture, the samples were placed on ice for 1 h. The samples were sonicated, and DNA fragments were combined with anti-Gli2 antibody (sc-271786, 1:100, Santa Cruz Biotechnology, CA, USA), anti-HDAC5 antibody (sc-133106, 1:200, Santa Cruz Biotechnology), anti-H3K9ac antibody (ab32129, 1:30, Abcam), anti-H3K14ac antibody (ab203952, 1:100, Abcam), and anti-H3K27ac antibody (ab4729, 1:50, Abcam) or IgG (ab205718, 1:1000, Abcam) antibody at 4 °C overnight. Then, 60 μL of Protein A/G beads were added to each tube for coupling and centrifugation. Each tube was eluted with 250 μL ChIP eluent, followed by DNA recovery and purification. Finally, qPCR was performed.

Dual-luciferase reporter assay

Dual-luciferase reporter assay was used to detect the specific binding sites of Gli2 and *Dram1* promoter. Dual-luciferase reporter gene vector containing the truncated sequences (Dram1-Luc1 (−2000 to −461), Dram1-Luc2 (−1682 to −461), Dram1-Luc3 (−493 to −461) and Dram1-Luc4 (-461-0)) were constructed. Cells were then co-transfected with sh-NC or sh-Gli2 with the above plasmids using Lipofectamine 2000 (Thermo Fisher Scientific). After 48 h, the cells were collected and luciferase activity was assessed using a luciferase reporter analysis system (Promega, Madison, WI, USA).

RT-qPCR assay

Total RNA was isolated from fresh brain tissues or cells using TRIzol reagent. The total RNA concentration was measured using an ultraviolet spectrophotometer. RNA was reversely transcribed into cDNA using the Superscript III Reverse Transcription Kit (Thermo Fisher Scientific). Gene expression was tested by TB Green ® Premix Ex Taq™ II (Takara, Dalian, China). Using GAPDH as an internal reference, the levels of Gli2, Dram1, and HDAC5 were counted using the $2^{-\Delta\Delta Ct}$ method. The primer sequences were listed below (5'-3'):

Gli2-F: GCCCTGGAGAGTCACCCTT
Gli2-R: TGCACAGACCGGAGGTAGT
Dram1-F: TCATCTCCTACGTGGTCGC
Dram1-R: CTGCGCCAAGAAATGCAGAG
HDAC5-F: TGCAGCACGTTTTGCTCCT
HDAC5-R: GACAGCTCCCCAGTTTTGGT
GAPDH-F: TGGATTTGGACGCATTGGTC
GAPDH-R: TTTGCACTGGTACGTGTTGAT

Western blotting

Cells and brain tissues were lysed with RIPA lysis buffer (Beyotime). Proteins were quantified using a BCA protein assay kit (Beyotime). Subsequently, the protein samples were subjected to SDS-PAGE for separation and then transferred onto PVDF membranes at 4 °C for 90 min (Millipore, Schwalbach, Germany). The membranes were blocked with 5% skim milk and incubated with primary antibody overnight at 4 °C. The membranes were then treated at 25 °C for 2 h with the secondary antibody of the corresponding species of the primary antibody, and protein bands were examined with a chemiluminescent substrate (Meilunbio, Dalian, China). Primary antibodies were as follows: anti-Gli2 (ab277800, 1:1000, Abcam),

anti-Dram1 (PA5-20335, 1:3000, Invitrogen), anti-PCA1 (PA5-109430, 1:5000, Invitrogen), anti-GOLPH3 (ab98023, 1:1000, Abcam), anti-ARF4 (ab190000, 1:1000, Abcam), anti-GM130 (G7295, 1:200, Sigma), anti-ACBD3 (PA5-116686, 1:2000, Invitrogen), anti-HDAC1 (ab280198, 1:1000, Abcam), anti-HDAC2 (ab32117, 1:2000, Abcam), anti-HDAC3 (ab32369, 1:5000, Abcam), anti-HDAC4 (ab235583, 1:1000, Abcam), anti-HDAC5 (ab55403, 1:500, Abcam) and anti-GAPDH (ab8245, 1:10000, Abcam).

Statistics and reproducibility

Statistical processing was performed using GraphPad Prism 8 software, and the experimental data were expressed as mean ± standard deviation (SD). For in vitro experiments, three biological replicates were performed, with each replicate consisting of triplicate technical repeats. For animal experiments, 6 mice per group were performed. The normality of data was assessed using the Shapiro-Wilk test. At a significance level of 5%, there were no significant deviations from the normality of all data ($P > 0.05$). Variance heterogeneity was detected using the F-test and Bartlett's test, and the variance of data was found to be equal. Two-tailed Student's *t* test was used to compare the differences between two groups, and one-way analysis of variance (ANOVA) with Tukey's post hoc test was performed to compare the differences between multiple groups. $P < 0.05$ indicated statistically significant.

Reporting summary

Further information on research design is available in the Nature Portfolio Reporting Summary linked to this article.

Data availability

The data that support the findings of this study are available from the corresponding author upon reasonable request.

Received: 13 November 2024; Accepted: 28 July 2025;
Published online: 13 August 2025

References

1. Mao, Z. et al. Ligustilide ameliorates hippocampal neuronal injury after cerebral ischemia reperfusion through activating PINK1/Parkin-dependent mitophagy. *Phytomedicine* **101**, 154111 (2022).
2. Chen, Y. et al. Srs11-92, a ferrostatin-1 analog, improves oxidative stress and neuroinflammation via Nrf2 signal following cerebral ischemia/reperfusion injury. *CNS Neurosci. Ther.* **29**, 1667–1677 (2023).
3. Lan, Z. et al. Curcumin-primed olfactory mucosa-derived mesenchymal stem cells mitigate cerebral ischemia/reperfusion injury-induced neuronal PANoptosis by modulating microglial polarization. *Phytomedicine* **129**, 155635 (2024).
4. Xu, D. et al. Orexin-A alleviates astrocytic apoptosis and inflammation via inhibiting OX1R-mediated NF-κB and MAPK signaling pathways in cerebral ischemia/reperfusion injury. *Biochim Biophys. Acta Mol. Basis Dis.* **1867**, 166230 (2021).
5. Huang, Y. et al. UBIAD1 alleviates ferroptotic neuronal death by enhancing antioxidative capacity by cooperatively restoring impaired mitochondria and Golgi apparatus upon cerebral ischemic/reperfusion insult. *Cell Biosci.* **12**, 42 (2022).
6. Xiaowei, X., Qian, X. & Dingzhou, Z. Sirtuin-3 activates the mitochondrial unfolded protein response and reduces cerebral ischemia/reperfusion injury. *Int J. Biol. Sci.* **19**, 4327–4339 (2023).
7. He, J. et al. OM-MSCs Alleviate the Golgi Apparatus Stress Response following Cerebral Ischemia/Reperfusion Injury via the PEDF-PI3K/Akt/mTOR Signaling Pathway. *Oxid. Med Cell Longev.* **2021**, 4805040 (2021).
8. Meng, F. et al. A deuterohemin peptide protects cerebral ischemia-reperfusion injury by preventing oxidative stress in vitro and in vivo. *Exp. Cell Res* **422**, 113432 (2023).
9. Li, T. et al. GOLPH3 Mediated Golgi Stress Response in Modulating N2A Cell Death upon Oxygen-Glucose Deprivation and Reoxygenation Injury. *Mol. Neurobiol.* **53**, 1377–1385 (2016).
10. He, J. et al. Olfactory Mucosa Mesenchymal Stem Cells Alleviate Cerebral Ischemia/Reperfusion Injury Via Golgi Apparatus Secretory Pathway Ca(2+) -ATPase Isoform1. *Front Cell Dev. Biol.* **8**, 586541 (2020).
11. Fan, Y. et al. A New Approach of Short Wave Protection against Middle Cerebral Artery Occlusion/Reperfusion Injury via Attenuation of Golgi Apparatus Stress by Inhibition of Downregulation of Secretory Pathway Ca(2+)-ATPase Isoform 1 in Rats. *J. Stroke Cerebrovasc. Dis.* **25**, 1813–1822 (2016).
12. Sasaki, A. et al. Effects of trunk neuromuscular electrical stimulation on the motor circuits of able-bodied individuals. *Exp. Brain Res* **241**, 979–990 (2023).
13. Pan, Z. et al. The Effects of Repetitive Transcranial Magnetic Stimulation in Patients with Chronic Schizophrenia: Insights from EEG Microstates. *Psychiatry Res* **299**, 113866 (2021).
14. Liang, H. et al. Repetitive Transcranial Magnetic Stimulation Improves Neuropathy and Oxidative Stress Levels in Rats with Experimental Cerebral Infarction through the Nrf2 Signaling Pathway. *Evid. Based Complement Altern. Med* **2021**, 3908677 (2021).
15. Zong, X. et al. Theta-burst transcranial magnetic stimulation promotes stroke recovery by vascular protection and neovascularization. *Theranostics* **10**, 12090–12110 (2020).
16. Luo, L. et al. Intermittent theta-burst stimulation improves motor function by inhibiting neuronal pyroptosis and regulating microglial polarization via TLR4/NFκB/NLRP3 signaling pathway in cerebral ischemic mice. *J. Neuroinflammation* **19**, 141 (2022).
17. Han, B. et al. Perspectives and new aspects of histone deacetylase inhibitors in the therapy of CNS diseases. *Eur. J. Med Chem.* **258**, 115613 (2023).
18. Kumar, V., Kundu, S., Singh, A. & Singh, S. Understanding the Role of Histone Deacetylase and their Inhibitors in Neurodegenerative Disorders: Current Targets and Future Perspective. *Curr. Neuropharmacol.* **20**, 158–178 (2022).
19. Gomez-Sanchez, J. A. et al. Emerging Role of HDACs in Regeneration and Ageing in the Peripheral Nervous System: Repair Schwann Cells as Pivotal Targets. *Int. J. Mol. Sci.* **23**, https://doi.org/10.3390/ijms23062996 (2022).
20. Li, N. et al. Opposite effects of HDAC5 and p300 on MRTF-A-related neuronal apoptosis during ischemia/reperfusion injury in rats. *Cell Death Dis.* **8**, e2624 (2017).
21. Lv, H., Li, Y., Cheng, Q., Chen, J. & Chen, W. Neuroprotective Effects Against Cerebral Ischemic Injury Exerted by Dexmedetomidine via the HDAC5/NPAS4/MDM2/PSD-95 Axis. *Mol. Neurobiol.* **58**, 1990–2004 (2021).
22. Etiévant, A. et al. Repetitive transcranial magnetic stimulation induces long-lasting changes in protein expression and histone acetylation. *Sci. Rep.* **5**, 16873 (2015).
23. Chen, J. L., Chang, C. H. & Tsai, J. W. Gli2 Rescues Delays in Brain Development Induced by Kif3a Dysfunction. *Cereb. Cortex* **29**, 751–764 (2019).
24. Lin, J., Lin, Y., Zhu, S., Luo, J. & Zhou, C. Transplantation of Wnt3a-modified neural stem cells promotes neural regeneration and functional recovery after spinal cord injury via Wnt-Gli2 pathway. *Neuroreport* **35**, 27–36 (2024).
25. Xu, B.-L. et al. Inhibitory effect of main phenolic acid components of Jacobaea cannabifolia (Less.) on inflammation caused by PM2.5. *Front. Pharmacol.* **13**, https://doi.org/10.3389/fphar.2022.1096137 (2023).
26. Chen, L. et al. O-GlcNAcylation promotes cerebellum development and medulloblastoma oncogenesis via SHH signaling. *Proc. Natl Acad. Sci. USA* **119**, e2202821119 (2022).

27. Han, L., Pan, Y. & Wang, B. Small ubiquitin-like Modifier (SUMO) modification inhibits GLI2 protein transcriptional activity in vitro and in vivo. *J. Biol. Chem.* **287**, 20483–20489 (2012).
28. Chen, G. et al. Role of DRAM1 in mitophagy contributes to preeclampsia regulation in mice. *Mol. Med Rep.* **22**, 1847–1858 (2020).
29. Yu, M., Jiang, Y., Feng, Q., Ouyang, Y. & Gan, J. DRAM1 protects neuroblastoma cells from oxygen-glucose deprivation/reperfusion-induced injury via autophagy. *Int J. Mol. Sci.* **15**, 19253–19264 (2014).
30. Wei, M. et al. DRAM1 deficiency affects the organization and function of the Golgi apparatus. *Cell Signal* **63**, 109375 (2019).
31. Zhao, P. et al. TAT-PEP Alleviated Cognitive Impairment by Alleviating Neuronal Mitochondria Damage and Apoptosis After Cerebral Ischemic Reperfusion Injury. *Mol. Neurobiol.* **60**, 5655–5671 (2023).
32. Campbell, B. C. V. et al. Ischaemic stroke. *Nat. Rev. Dis. Prim.* **5**, 70 (2019).
33. Li, C. et al. Pleiotropic Microenvironment Remodeling Micelles for Cerebral Ischemia-Reperfusion Injury Therapy by Inhibiting Neuronal Ferroptosis and Glial Overactivation. *ACS Nano* **17**, 18164–18177 (2023).
34. Liu, L. et al. Integrin α3 is required for high-frequency repetitive transcranial magnetic stimulation-induced glutamatergic synaptic transmission in mice with ischemia. *CNS Neurosci. Ther.* **30**, e14498 (2024).
35. Zhou, L. et al. Current evidence, clinical applications, and future directions of transcranial magnetic stimulation as a treatment for ischemic stroke. *Front Neurosci.* **17**, 1177283 (2023).
36. Zhang, Y. et al. Golgi Stress Response, Hydrogen Sulfide Metabolism, and Intracellular Calcium Homeostasis. *Antioxid. Redox Signal* **32**, 583–601 (2020).
37. Liu, J. et al. The role of the Golgi apparatus in disease (Review). *Int. J. Mol. Med.* **47**, https://doi.org/10.3892/ijmm.2021.4871 (2021).
38. Zhang, Y. & Seemann, J. Rapid degradation of GRASP55 and GRASP65 reveals their immediate impact on the Golgi structure. *J Cell Biol* **220**, https://doi.org/10.1083/jcb.202007052 (2021).
39. Li, J., Ahat, E. & Wang, Y. Golgi Structure and Function in Health, Stress, and Diseases. *Results Probl. Cell Differ.* **67**, 441–485 (2019).
40. Li, Z., Zhang, W., Xu, J. & Mo, X. Cdk1 protects against oxygen-glucose deprivation and reperfusion-induced Golgi fragmentation and apoptosis through mediating GM130 phosphorylation. *J. Mol. Histol.* **54**, 609–619 (2023).
41. Nozaki, Y. et al. The effects of WWP1 overexpression on the golgi apparatus stress response and proteoglycan production in adipocytes. *Sci. Rep.* **14**, 29004 (2024).
42. Sohda, M. et al. Identification and characterization of a novel Golgi protein, GCP60, that interacts with the integral membrane protein giantin. *J. Biol. Chem.* **276**, 45298–45306 (2001).
43. Shirai, R. et al. FTD/ALS Type 7-Associated Thr104Asn Mutation of CHMP2B Blunts Neuronal Process Elongation, and Is Recovered by Knockdown of Arf4, the Golgi Stress Regulator. *Neurol. Int* **15**, 980–993 (2023).
44. Yamaguchi, H. et al. Wipi3 is essential for alternative autophagy and its loss causes neurodegeneration. *Nat. Commun.* **11**, 5311 (2020).
45. Chen, F., Han, J. & Wang, D. Identification of key microRNAs and the underlying molecular mechanism in spinal cord ischemia-reperfusion injury in rats. *PeerJ* **9**, e11454 (2021).
46. Jiang, R. et al. METTL3 stabilizes HDAC5 mRNA in an m(6)A-dependent manner to facilitate malignant proliferation of osteosarcoma cells. *Cell Death Discov.* **8**, 179 (2022).
47. Formisano, L. et al. HDAC4 and HDAC5 form a complex with DREAM that epigenetically down-regulates NCX3 gene and its pharmacological inhibition reduces neuronal stroke damage. *J. Cereb. Blood Flow. Metab.* **40**, 2081–2097 (2020).
48. Wang, C., Chen, R., Zhu, X. & Zhang, X. Suberoylanilide Hydroxamic Acid Ameliorates Pain Sensitization in Central Neuropathic Pain After Spinal Cord Injury via the HDAC5/NEDD4/SCN9A Axis. *Neurochem Res* **48**, 2436–2450 (2023).
49. Long, X. et al. Astrocyte-derived exosomes enriched with miR-873a-5p inhibit neuroinflammation via microglia phenotype modulation after traumatic brain injury. *J. Neuroinflammation* **17**, 89 (2020).
50. Li, H. et al. Repetitive Transcranial Magnetic Stimulation Alleviates Neurological Deficits After Cerebral Ischemia Through Interaction Between RACK1 and BDNF exon IV by the Phosphorylation-Dependent Factor MeCP2. *Neurotherapeutics* **17**, 651–663 (2020).
51. Hong, Y. et al. High-frequency repetitive transcranial magnetic stimulation improves functional recovery by inhibiting neurotoxic polarization of astrocytes in ischemic rats. *J. Neuroinflammation* **17**, 150 (2020).

Acknowledgements

This work was supported by National Natural Science Foundation of China (82460456).

Author contributions

Chunjiao Zhu: Conceptualization; Validation; Investigation; Resources; Writing-Original Draft; Yongmei Fan: Supervision; Methodology; Formal analysis; Data Curation; Visualization; Wenna Peng: Writing-Review & Editing; Project administration; Funding acquisition.

Competing interests

The authors declare no competing interests.

Additional information

Supplementary information The online version contains supplementary material available at https://doi.org/10.1038/s42003-025-08613-8.

Correspondence and requests for materials should be addressed to Wenna Peng.

Peer review information *Communications Biology* thanks Lixuan Zhan, Qun Fu, and the other, anonymous, reviewer for their contribution to the peer review of this work. Primary Handling Editors: Tobias Goris and Joao Manuel de Sousa Valente.